Effects of Distal Pocket Mutations on the Geminate Recombination of NO with Leghemoglobin on the Picosecond Time Scale

P. K. Chowdhury,[†] S. Kundu,[‡] M. Halder[†], K. Das,[†,||] M. S. Hargrove,*[,‡] and J. W. Petrich*[,†]

Departments of Chemistry and of Biochemistry, Biophysics, and Molecular Biology, Iowa State University, Ames, Iowa 50011

Received: January 27, 2003; In Final Form: May 12, 2003

The picosecond NO geminate rebinding kinetics of wild-type leghemoglobin, a monomeric plant hemoglobin with structural similarity to myoglobin, and six mutant proteins at the distal histidine (H61G, H61A, H61V, H61L, H61R, H61F) are investigated. All of the mutant proteins yield rebinding kinetics that are initially more rapid than that of the wild-type protein. At long times, the rebinding of H61F becomes slower than that of wild-type leghemoglobin. The H61V, H61L, and H61G mutant proteins give extraordinarily rapid and complete geminate rebinding. On a 40 ps time scale, distal effects are overwhelmingly evident for all of the mutants considered. That binding is both rapid and, in several cases, essentially single-exponential is suggestive of the nature of the barrier induced by the distal modification: it must be such that the ligand is prohibited from reorienting with respect to, and diffusing sufficiently far from, the heme iron so that a distribution of return paths is not offered to it. Over the past 20 years, the relative importance attributed to the proximal and the distal sides in modulating geminate ligand binding has varied considerably. Our results with leghemoglobin are discussed in terms of the relative contributions of proximal and distal effects to geminate rebinding kinetics.

Introduction

Site-directed mutagenesis and recombinant protein technology coupled with ever-increasing improvements in computational, structural, and kinetic studies has provided a considerable increase in our understanding of ligand binding in myoglobin (Mb) itself. A study of Mb alone, however, cannot provide a completely satisfying paradigm for understanding more complicated heme proteins, such as newly discovered bacterial, protist, and plant hemoglobins and flavohemoglobins, or, for that matter, even human hemoglobin.[1−4] The study of leghemoglobins ideally complements that of myoglobin because, despite a structure (Figure 1) similar to that of Mb, they display many opposite extremes of reactivity.[5−7]

When ligands bound to a hemoglobin are photolyzed, the resulting time courses for rebinding are often complex and depend on a number of factors including (1) reactivity of the heme iron with the ligand, (2) reactivity of the ligand, and (3) the protein matrix surrounding the ligand binding site. A relatively long laser flash (microsecond duration) is used to study the overall bimolecular association reaction, which is influenced by each of the factors listed above. Shorter pulse durations (femtoseconds to nanoseconds) are used to probe geminate recombination that occurs when the dissociated ligand rebinds without exiting the protein matrix. Depending on the combination of the hemoglobin and the ligand, geminate recombination can occur on ultrafast (<10 ps) and a number of longer (10 ps to 10 μs) time scales.

Traditionally, the longer time scale experiments were thought to probe the distal heme pocket environment surrounding the ligand binding site, while the femtosecond to picosecond time scale components measured more directly the reactivity of the heme iron as monitored by the rate of bond formation and heme−His(F8) relaxations. However, because ∼10 ps geminate recombination has been observed with very few hemoglobins, this assumption has never been thoroughly tested.

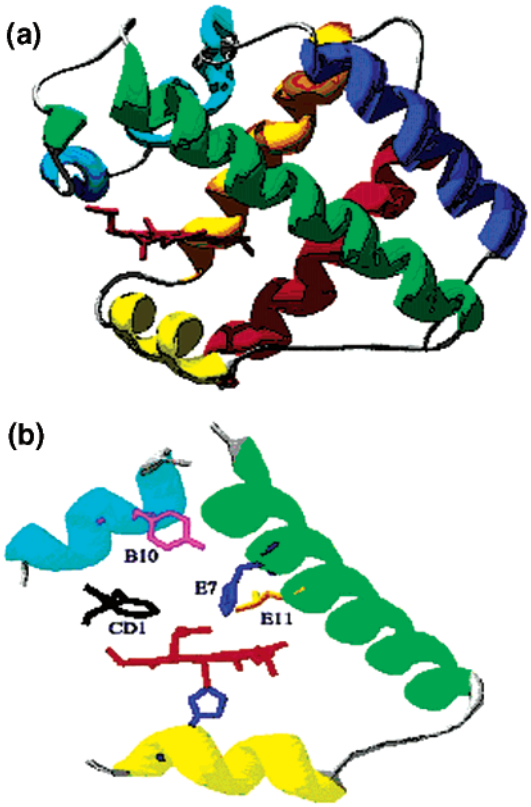

Figure 1. (a) Structure of the globin fold of leghemoglobin. (b) A closer look at the distal pocket of leghemoglobin and the histidine (E7) residue, which has been replaced by several other amino acids to study the effect of distal pocket mutations.

* To whom correspondence should be addressed. E-mail: msh@iastate.edu (M.S.H.); jwp@iastate.edu (J.W.P.).
[†] Department of Chemistry.
[‡] Department of Biochemistry, Biophysics, and Molecular Biology.
[||] Present address: Biomedical Applications Section, CAT, Indore, India.

10.1021/jp030106r CCC: $25.00
Published on Web 08/06/2003

Arguments for Proximal Effects in Geminate Recombination. Early investigations on fast geminate recombination, notably with NO, focused largely on proximal effects.[8,9] These studies were approached from the point of view of understanding *hemoglobin* (Hb), not myoglobin, and were motivated by the work of Perutz[10] and Gelin and Karplus[11] pointing to an allosteric core consisting of the heme, the proximal histidine, the F helix, and the FG corner, which is in contact with the $\alpha_1\beta_2$ interface. The response of this proximal heme environment to ligand dissociation and rebinding is expected to be significantly different in Mb and Hb.

The behavior of the proximal side can be monitored by means of the stretching frequency of the Fe−His mode in photodissociated MbCO and HbCO. The frequency of this mode is the same at 30 ps in the MbCO photoproducts as in equilibrium unligated Mb.[12] In the HbCO photoproduct, however, the frequency of the mode does not begin to change for several nanoseconds,[13,14] indicating an interaction of the proximal side with the interface between subunits. Friedman et al.[15] correlated the frequency of the Fe−His mode with the yield of O_2 geminate recombination in Hb and suggested that the degree of relaxation of the proximal side controls the reactivity of the protein. More recently, Friedman and co-workers have considered proximal effects in terms of both the Fe−His mode and the band III absorption (a charge-transfer band at ∼760 nm peculiar to 5-coordinate ferrous hemes).[16]

The importance of the proximal Fe−His mode motivated our earlier consideration of the ultrafast rebinding in terms of a transient barrier depending on the fluctuating out-of-heme plane displacement of the Fe following ligand dissociation.[9] This study examined the geminate rebinding kinetics in terms of various models: single exponential, sum of two exponentials, power law, and time-dependent barrier corresponding to the evolution of the heme iron. Although different functional forms could not unambiguously describe the ligand binding kinetics, the time scale of ligand rebinding was consistent with molecular dynamics simulations of the Fe−heme motion. This study therefore concluded that an out-of-plane configuration of the Fe with respect to the heme macrocycle reduces the rate of geminate binding, and that modulation of the Fe−heme distance on the time scale of geminate rebinding induces nonexponential rebinding kinetics.[9]

Arguments for Distal Effects in Geminate Recombination. Subsequent work has indicated that this view of the role of the proximal environment, *at least in monomeric heme proteins*, requires reassessment. Our ultrafast study of the NO geminate rebinding of a wide spectrum of distal mutants of human myoglobin demonstrated that distal effects can profoundly influence the kinetics.[17] For example, not only do the distal mutant proteins V68N, V68A, and H64Q exhibit rapid rebinding compared to wild-type Mb, but so does the surface mutant protein K45R. (K45R is at the interface of the heme pocket and solvent and interacts with a propionate. It could affect the pathway for ligand entry or exit.) On the other hand, the mutants K45A and K45Q yield kinetics almost identical to that of the wild type. Gibson, Olson, and co-workers[18,19] have obtained results consistent with these.

Work by Hochstrasser and co-workers[20] has also confirmed the importance of distal effects in sperm whale myoglobin. V68F and V68I have significantly smaller and larger time constants, respectively, for geminate rebinding with NO. They have also shown that Co substitution produces much less pronounced effects on NO geminate recombination with Mb than do distal pocket mutations.[20] The Co-substituted myoglobins, nevertheless, do provide slightly faster rebinding kinetics than do their Fe-bearing counterparts, which is indeed consistent (although possibly fortuitously) with a smaller out-of-plane displacement for Co than for Fe, and with the role of the displacement proposed by Petrich et al.[9] (discussed above).

Négrerie et al.[21] have studied NO geminate recombination in Mb in which the proximal histidine is mutated to glycine, thus furnishing a protein without covalent attachment to the heme iron. At sufficiently high imidazole concentration, the H93G mutant coordinates an imidazole at the proximal position of the heme, which is denoted as H93G(Im). This system consequently provides a means of assessing the contribution of proximal effects to geminate ligand rebinding. The mutation induces a relatively minor perturbation with respect to wild-type Mb (Table 2). The H93G(Im) kinetics is very similar to that of wild-type Mb, with the amount of rapid rebinding component being 42% and 45%, respectively. Surprisingly, the fraction of NO rebound after ∼100 ps is larger in the wild type than in the mutant protein, as is indicated by the relative weights of the "baseline" components, a_3. The amount of rapid rebinding in H93G, 63%, is more pronounced than in wild-type Mb.

Franzen et al.[22,23] demonstrated that the intensity of the Fe−His vibrational mode characteristic of heme doming was fully developed 1 ps after photodissociation of CO, within their experimental resolution, for both Mb and H93G(Im). (The intensity of this mode in Hb was also fully developed, but its frequency was upshifted with respect to its equilibrium value. Those of Mb and H93G(Im) were found to be at their equilibrium value 1 ps after CO photolysis.) Subsequent work by Mizutani and Kitigawa[24] with improved signal-to-noise ratio is consistent with these observations, but indicates that Mb and a model heme compound lacking the protein matrix show ∼90% of the intensity of the Fe−His mode within their instrumental response time of ∼2 ps, while the remainder develops with a time constant of a few picoseconds. These workers also detect a small evolution (∼2 cm^{-1}) of the frequency of this mode occurring on a 100 ps time scale. These results indicate that the proximal protein environment, at least in monomeric hemoglobins, seems to have a relatively minor effect on the Fe−His mode. In this context, then, it is not surprising that proximal effects on geminate binding are generally small relative to distal effects.

Négrerie et al.[21] have recently studied soluble guanylate cyclase (sGC), in which the binding of NO to the heme iron induces a cleavage of the bond between the proximal histidine and the iron. sGC−NO is an example of a heme protein where there is no covalent attachment between the Fe and the proximal side of the protein, and its kinetics may thus be compared against other systems in evaluating distal and proximal effects on geminate rebinding. sGC exhibits very rapid NO geminate binding kinetics, 97% of the recombination occurring with a time constant of 7.5 ps. Given that NO binds to protoheme with a 7 ps time constant (Table 1) and that H93G Mb is only moderately different with respect to wild-type Mb, Négrerie et al. concluded that their sGC result implies that rapid, single-exponential rebinding behavior is not a consequence of proximal behavior, but of the distal environment.

Magde and co-workers investigated NO geminate binding kinetics in horse heart and sperm whale myoglobin at pH 4.[25] Under these conditions, the proximal histidine−iron bond is broken, providing a local heme environment similar to that of sGC−NO. These workers observed single-exponential NO rebinding kinetics with time constants of 12.5 and 9.5 ps, respectively (Table 1). Although it is tempting to interpret these

results as supporting the hypothesis[9] concerning the importance of the proximal effects exerted by the Fe−heme displacement, the protein may be sufficiently altered at pH 4[26−28] so that these results more readily confirm the conclusions of Négrerie et al. based on their sGC−NO data.

Distal and Proximal Effects in Leghemoglobins. The first ultrafast NO geminate rebinding study directly addressing proximal effects in leghemoglobin (Lba) and myoglobin mutants[6] indicated that these effects are negligible in Mb up to ~900 ps after photodissociation (in S92V and a Lba F-helix substitution). In Lba systems (V91S and a Mb F-helix substitution), proximal effects are negligible on a 40-ps time scale. On the other hand, they are "small" but clearly evident on a 1-ns time scale. This and the present study provide the first systematic investigations of the role of proximal and distal effects on the "ultrafast" geminate recombination of NO with Lba. The results presented here point to considerable distal effects that manifest themselves in the first tens of picoseconds following photodissociation and are consistent with distal heme pocket regulation of geminate recombination.

Materials and Methods

Preparation of NO-Bound Lba Samples for Geminate Recombination Measurements. The mutagenesis, expression, and purification of the Lba proteins employed is reported in detail elsewhere.[5] The myoglobin mutants discussed are from sperm whale. The NO-complexed protein samples were prepared in a cuvette (1 mm path length) stoppered with a septum in an oxygen-free atmosphere. LbCO samples were prepared by reducing the proteins with sodium dithionite and loading them into a Sephadex G-25 size exclusion column equilibrated with 100 mM phosphate, pH 7.0, saturated in CO (10% CO, 90% N_2 mixture). The dithionite-free, ligand-bound samples were collected in gastight syringes. Ferrous NO samples were made by diluting these dithionite-free CO samples 1:1 with NO-saturated anaerobic buffer. The absorption spectra of the NO forms of the wild-type proteins and their mutants used in this study are nearly identical. The protein samples typically had an absorbance of ~0.5 at 407 nm.

Measurement and Analysis of Geminate Recombination Kinetics. The laser apparatus used for pump−probe transient absorption measurements used in the geminate recombination studies has been described in detail elsewhere.[29] In brief, a 1 kHz homemade, regeneratively amplified Ti:sapphire laser was used to photolyze the sample at 407 nm with an energy of 1 μJ per pulse. A white light continuum was then used to probe the absorption changes at 438 nm. To facilitate the comparison of data for various mutants, the absorbance changes were normalized to 1 at the maximum change in absorbance. Sample integrity was monitored by measuring the absorption spectra before the start of and after the completion of each experiment. The kinetics on the 40 ps time scale were fit globally according to the following function: $\Delta A(t) = a_1 \exp(-t/\tau_1) + a_2 \exp(-t/\tau_2)$. That is, τ_2, effectively infinite on this time scale, was held fixed while τ_1 and the amplitudes, a_1 and a_2, were allowed to vary until the best fits were obtained. On longer time scales, a simple sum of exponentials was used. An alternative, model-independent means of analyzing the data is to fit the kinetic traces to a distribution of rebinding rates. Such an analysis has been applied on several occasions to geminate rebinding of NO.[17,21,30] This method obtains the rate distributions from the kinetic curves by using the maximum entropy method (MEM). In this approach, an entropy function is maximized and a distribution of probabilities of the underlying rate components is obtained. The resulting distribution is the most probable, but not unique, rate distribution describing the observed kinetics.[31−33] Self-consistency checks for the use of the maximum entropy method are (1) that the fit to the MbCO rebinding kinetics yields only time constants that are smaller than the time scale of the experiment (not shown), (2) that the ultrafast NO rebinding of, for example, the H61L Lb mutant yields a single narrow peak in the rate distribution, and (3) that superimposable (within the experimental noise) kinetic traces of different mutants yield similar distributions of recombination rates. The maxima of the MEM distributions were normalized to unity to facilitate comparison among the mutant proteins.

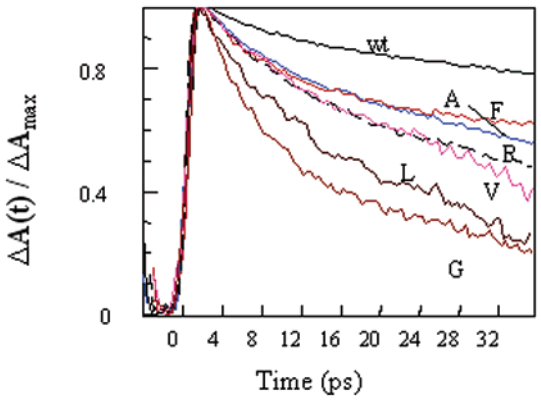

Figure 2. An overlay of the room-temperature decay curves (NO geminate recombination) of the wild-type protein (wtLb) and its corresponding distal mutant proteins, where wt stands for wtLb and the letters F, A, R, V, L, and G stand for the mutant proteins H61F, H61A, H61R, H61V, H61L, and H61G, respectively. Decays collected on a 40 ps time scale are displayed. The samples were photodissociated at 407 nm and probed at 438 nm.

Bimolecular Recombination Kinetics. The association rate constants for bimolecular NO binding were measured by laser photolysis methods[34,35] using a previously described laser flash apparatus.[36] All kinetic measurements were taken at 25 °C in 100 mM phosphate, pH 7.0. The NO rebinding after photolysis was followed at 428 nm (the deligated peak for Lba). The kinetic traces are single-exponential, and a suitable curve fitting yields the rate constants. The dissociation rate constants were measured with a Cary 50-Bio spectrophotometer by displacing bound NO with CO in the presence of dithionite. Error estimates for the rate constants are ~±10% of the measured value.

Results and Discussion

Figures 2 and 3 present geminate recombination kinetics on time scales of 40 and 400 ps, respectively, for the six distal mutant proteins and wild-type Lba. It is remarkable that for H61G, H61V, and H61L the rebinding is more than 80% complete within 80 ps after NO photolysis. Such efficient geminate recombination is comparable to that of protoheme−NO in ethylene glycol water,[8] myoglobin at pH 4,[25] and soluble guanylate cyclase,[21] which afford the most rapid and complete rebinding of which we are aware. Tables 1−3 summarize these geminate and bimolecular rebinding parameters.

As noted earlier, the first ultrafast NO geminate rebinding study directly addressing proximal effects in leghemoglobin and myoglobin mutants[6] indicated that they are negligible in Mb up to ~900 ps after photodissociation (in S92V and an Lba F-helix substitution, Figure 3A). In Lba systems (V91S and an Mb F-helix substitution), proximal effects are negligible on a 40 ps time scale. On the other hand, they are "small" but clearly evident on a 1 ns time scale (Figure 3A). The present work

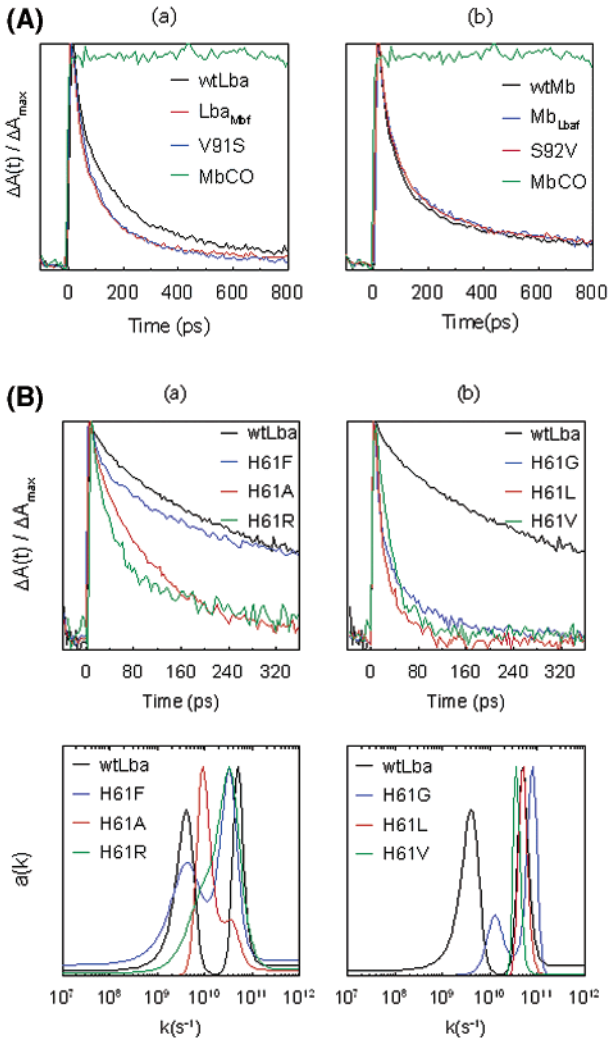

Figure 3. (A) (a) Kinetic traces (1 ns full time scale) for wtLba and its proximal mutants. (b) Kinetic traces (1 ns full time scale) for wtMb and its proximal mutants. The mutant proteins S92VMb and V91SLba were selected, as discussed in detail elsewhere, because they are complimentary substitutions resulting in an Lba-like proximal pocket in Mb (S92V) and an Mb-like proximal pocket in Lba (V91S).[6] (B) For the two panels (a) and (b), the top portion represents the kinetic traces (400 ps full time scale) and the bottom the corresponding distributions for wtLba and its distal mutants obtained from MEM analysis.

points to considerable distal effects that manifest themselves in the first tens of picoseconds following photodissociation. To a first approximation, we might conclude that proximal or distal effects on ligand binding are a direct consequence of structural factors on the respective sides of the heme—although, the situation may be more complicated, as we suggest below.

The geminate rebinding of the distal mutants of leghemoglobin considered in the present work can be fruitfully considered in light of an analysis of rate distributions. The mutant proteins fall into two classes. The kinetic data obtained on a 400 ps time scale indicate bimodal distributions for wild-type leghemoglobin and for its mutants, notably H61A and H61F (Figure 3B). While the two lobes for the wild-type distribution are well separated and of comparable amplitude, those for the H61A and the H61F mutants are closer, with the lower amplitude lobes appearing as shoulders in the distributions. It is interesting that the shoulder for H61A occurs at larger rate constants compared to that for H61F, which occurs at smaller rate constants. In marked contrast, the distributions for the H61V and the H61L mutant proteins display one band, which is narrow and sharply peaked at large rate constants, consistent with the rapid, nearly single-exponential rebinding kinetics (Figure 3).

TABLE 1: NO Geminate Rebinding Kinetic Parameters of the Fe(II) Forms of Soybean Lba, Its Distal Mutant Proteins, and Others

sample	a_1[a]	τ_1 (ps)	sample	a_1[a]	τ_1 (ps)
wild-type Lba	0.23	27	Lba H61V	0.67	21
Lba H61A	0.49	19.5	PTH−NO[b]	0.92	7
Lba H61R	0.59	17	guanylate cyclase[c]	0.97	7.5
Lba H61G	0.80	11	sperm whale Mb, pH 4[d]	1.00	9.5
Lba H61L	0.90	21	horse heart Mb, pH 4[d]	1.00	12.5
Lba H61F	0.38	11			

[a] Unless otherwise indicated, fitting results for geminate rebinding kinetics were obtained on a full scale of 40 ps. Kinetics are globally fit, as discussed in the text, to the form $\Delta A(t) = a_1 \exp(-t/\tau_1) + a_2 \exp(-t/\tau_2)$, where τ_2 is too long to be fit accurately on this time scale and is effectively infinite. τ_2 is fixed at 2 ns for the global fits. The prefactors are normalized such that $a_1 + a_2 = 1$. [b] PTH (protoheme) in ethylene glycol/water (95:5). The kinetics are cited from ref 9. λ_{pump} = 580 nm, and λ_{probe} = 425 nm. [c] Soluble guanylate cyclase.[21] [d] Reference 25.

TABLE 2: Fit Parameters for Picosecond NO Geminate Rebinding Data Obtained on Longer Time Scales: Distal and Proximal Effects

protein	a_1[a]	τ_1 (ps)	a_2	τ_2 (ps)	a_3
wt Mb	0.19	30	0.57	150	0.24
wt Lba	0.12	20	0.62	190	0.26
Lba H61A	0.19	11	0.80	114	0.01
Lba H61R	0.60	25	0.35	150	0.05
Lba H61G	0.75	15	0.25	105	
Lba H61L	0.48	5	0.52	30	
Lba H61F	0.22	12	0.48	170	0.30
wt Mb[b]	0.45	11	0.50	92	0.05
Mb H93G(Im)[b]	0.42	14.7	0.39	82	0.19
Mb H93G[b]	0.63	14.6	0.25	95	0.12

[a] Unless otherwise indicated, the fits reported are for data obtained on a full scale of 400 ps. [b] Sperm whale myoglobin and its proximal histidine mutant. See the discussion in the text. The data were obtained on a full scale of 100 ps.[21]

TABLE 3: Bimolecular Rate Constants for Wild-Type Lba and Its Mutants[a]

protein	k'_{NO} (μM^{-1} s^{-1})	k_{NO} (s^{-1})	K_{NO} (μM^{-1})
wt Lb	190	0.00002	9000000
H61G	330	0.00002	17000000
H61A	300	0.00002	15000000
H61V	230	0.00002	12000000
H61L	320	0.00002	16000000
H61F	360	0.0001	3600000
H61R	310	0.00001	31000000

[a] k'_{NO} are association rate constants, k_{NO} dissociation rate constants, and K_{NO} affinity constants (k'_{NO}/k_{NO}). Errors in the rate constants are approximately ±10% of the measured value.

The first bimolecular recombination kinetic data of leghemoglobin and its mutants are presented in Table 3 and in Figure 4 for purposes of comparison. The rebinding kinetics are well described by a single exponential as is indicated by the representative kinetic traces and MEM fits and distributions. The availability of the bimolecular data provides a useful perspective from which to evaluate the geminate data. For example, among the proteins studied, the H61F mutant protein has the largest bimolecular rebinding rate constant and about the smallest geminate rebinding rate constant. These two observations can be reconciled if it is postulated that the mutation introduces an opening in the heme pocket, which, while

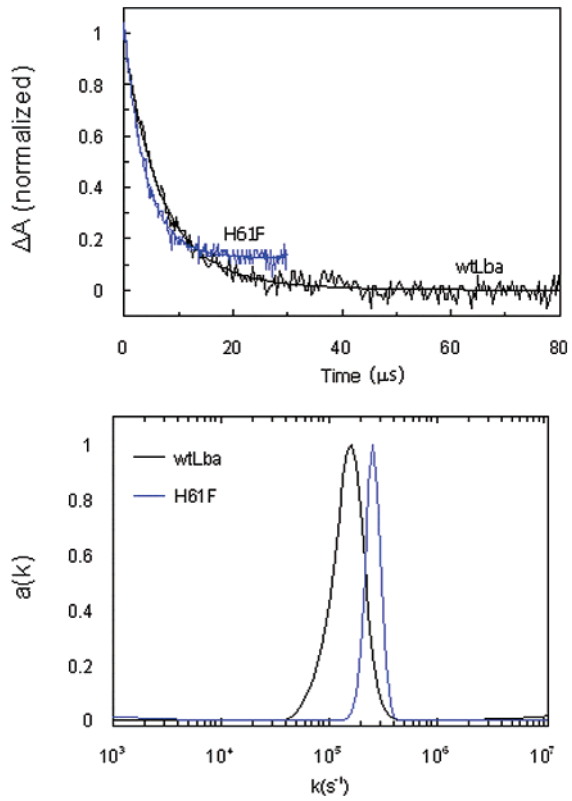

Figure 4. Bimolecular rebinding of NO to wild-type leghemoglobin and H61F and the corresponding MEM fits and distributions.

permitting the ligand to stray further from the Fe (thus providing slow geminate rebinding), also permits easy reentry for ligands that have already exited (fast bimolecular rebinding). Such an opening also explains the ~5-fold higher dissociation rate constant in H61F, as opposed to the other mutant proteins (Table 3). On the other hand, the lower NO dissociation rate constant in H61R might be a result of strong hydrogen bonds with the bound ligand.[5]

Similarly, if the rate of geminate ligand rebinding is enhanced, it must be because the barrier to ligand diffusion away from the heme has been increased, and vice versa. In addition, slow geminate rebinding may be the result of stabilization of the ligand by interactions with amino acids in the pocket—i.e., a so-called "docking site". "Docking" for CO in Mb has been indicated in spectroscopic[37] and structural[38] studies. For example, it has long been considered that the rapid geminate rebinding of nitric oxide with heme proteins is a consequence of a very small electronic barrier for heme rebinding relative to that of oxygen or carbon monoxide.[9,17,20,39−41] The origin of this rapid rebinding has been called into question by Anfinrud and co-workers, who have attributed it to distal effects. They compared the rebinding of CO with Mb and with microperoxidase. Microperoxidase is an enzymatically digested cytochrome *c* oxidase consisting of a heme with a "proximal" histidine, which is part of an 11-peptide fragment. This peptide is not long enough to wrap around the heme to form an organized distal environment. CO recombination with microperoxidase is very rapid, with an initial component of 110 ps and with more than 80% of the ligands being re-bound after 1 ns. One nanosecond after photodissociation, essentially no CO has recombined with Mb.[37] In this context, the rapid NO recombination observed in the H61V, H61L, and H61G leghemoglobin mutants could be explained in terms of a reduction of attractive forces between the distal docking site residues and the NO.

Finally, it may be overly simplistic to distinguish between proximal effects independently of distal effects. It is possible that certain proximal mutations may influence the distal barrier. It is also possible, as suggested by the simulations of Lambry,[42] that the trajectory of the dissociated ligand causes it to collide with the distal pocket in such a way that fluctuations in the heme pocket are very rapidly set into motion, subsequently influencing the rebinding kinetics.

Conclusions

We have presented the first ultrafast spectroscopic study addressing the distal effects on the geminate recombination of NO with leghemoglobin and its mutants. The H61V, H61L, and H61G mutant proteins show extraordinarily rapid and complete geminate rebinding, approaching that exhibited by PTH−NO, myoglobin at pH 4, and guanylate cyclase (Table 1). The picosecond NO geminate rebinding kinetics of wild-type leghemoglobin and six of its mutant proteins at the distal histidine-61 (H61G, H61A, H61V, H61L, H61R, H61F) have been investigated. All of the proteins yield rebinding kinetics that are initially more rapid that that of the wild type. At long times, the rebinding of H61F becomes slower than that of the wild type. The H61V, H61L, and H61G mutants give extraordinarily rapid and complete geminate rebinding. No distal or proximal mutations decrease the initial rate of geminate rebinding in leghemoglobin, and no mutations in myoglobin decrease the initial rate without at the same time permitting the ligand to escape to the solvent.[18]

A growing body of data support the importance of distal effects for inducing rapid, essentially single-exponential geminate rebinding in monomeric heme proteins. That suggests that the distal barrier prohibits the ligand from reorienting or diffusing very far from the heme iron, so that a distribution of return paths is not offered to it.

While proximal effects can be induced (ref 6 and Table 2), they are not as dramatic as distal modifications. Also, the data indicate that, in monomeric proteins, the role of the displacement of the Fe out of the heme plane is much less important than previously believed. A complete assessment, however, of proximal effects must await a prudent consideration of multimeric proteins exhibiting cooperativity before general conclusions are drawn concerning their importance. Finally, it may be overly simplistic to distinguish between proximal effects independently of distal effects. It is possible that certain proximal mutations may influence the distal barrier or that the distal barrier is influenced by the impact of the dissociated ligand.

Acknowledgment. This work was supported by NSF Grant MCB-0077890 to M.S.H. and J.W.P. We thank Michel Négrerie and Jean-Christophe Lambry for very helpful discussions and Andrew Shreve and Stefan Franzen for providing us the maximum entropy method software.

References and Notes

(1) Ermler, U.; Siddiqui, R.; Cramm, R.; Friedrich, B. *EMBO J.* **1995**, *14*, 6067.
(2) Gardner, P. R.; Gardner, A. M.; Martin, L. A.; Salzman, A. L. *Proc. Natl. Acad. Sci. U.S.A.* **1998**, *95*, 10378.
(3) Hargrove, M.; Brucker, E.; Stec, B.; Sarath, G.; Arredondo-Peter, R.; Klucas, R.; Olson, J.; Phillips, G. *Struct. Folding Des.* **2000**, *8*, 1005.
(4) Pesce, A.; Couture, M.; Dewilde, S.; Guertin, M.; Yamauchi, K.; Ascenzi, P.; Moens, L.; Bolognesi, M. *EMBO J.* **2000**, *19*, 2424.
(5) Kundu, S.; Hargrove, M. S. *Proteins* **2002**, *50*, 239.
(6) Kundu, S.; Snyder, B.; Das, K.; Chowdhury, P.; Park, J.; Petrich, J. W.; Hargrove, M. S. *Proteins* **2002**, *46*, 268.
(7) Gibson, Q. H.; Wittenberg, J. B.; Wittenberg, B. A.; Bogusz, D.; Appleby, C. A. *J. Biol. Chem.* **1988**, *264*, 100.

(8) Petrich, J. W.; Poyart, C.; Martin, J. L. *Biochemistry* **1988**, *27*, 4049.

(9) Petrich, J. W.; Lambry, J. C.; Kuczera, K.; Karplus, M.; Poyart, C.; Martin, J. L. *Biochemistry* **1991**, *30*, 3975.

(10) Perutz, M. F. *Mechanisms of Cooperativity and Allosteric Regulation in Proteins*; Cambridge University Press: Cambridge, 1990.

(11) Gelin, B. R.; Karplus, M. *Proc. Natl. Acad. Sci. U.S.A.* **1977**, *74*, 801.

(12) Findsen, E. W.; Friedman, J. M.; Ondrias, M. R.; Simon, S. R. *Science* **1985**, *229*, 661.

(13) Scott, T. W.; Friedman, J. M. *J. Am. Chem. Soc.* **1984**, *106*, 5677−5687.

(14) Shelnutt, J. A.; Rousseau, D. L.; Friedman, J. M.; Simon, S. R. *Proc. Natl. Acad. Sci. U.S.A.* **1979**, *76*, 4409.

(15) Friedman, J. M.; Scott, T. W.; Fisanick, G. J.; Simon, S. R.; Findsen, E. W.; Ondrias, M. R.; Macdonald, V. W. *Science* **1985**, *229*, 187.

(16) Ahmed, A. M.; Campbell, B. F.; Caruso, D.; Chance, M. R.; Chavez, M. D.; Courtney, S. H.; Friedman, J. M.; Iben, I. E. T.; Ondrias, M. R.; Yang, M. *Chem. Phys.* **1991**, *158*, 329.

(17) Petrich, J. W.; Lambry, J.-C.; Balasubramanian, S.; Lambright, D. G.; Boxer, S. G.; Martin, J. L. *J. Mol. Biol.* **1994**, *238*, 437.

(18) Carlson, M. L.; Regan, R.; Elber, R.; Haiying, L.; Phillips, G. N., Jr.; Olson, J. S.; Gibson, Q. H. *Biochemistry* **1994**, *33*, 10597.

(19) Gibson, Q. H.; Regan, R.; Elber, R.; Olson, J. S.; Carver, T. E. *J. Biol. Chem.* **1992**, *267*, 22022.

(20) Kholodenko, Y.; Gooding, E.; Dou, Y.; Ikeda-Saito, M.; Hochstrasser, R. *Biochemistry* **1999**, *38*, 5918.

(21) Négrerie, M.; Bouzhir, L.; Martin, J.-L.; Liebl, U. *J. Biol. Chem.* **2001**, *276*, 46815.

(22) Franzen, S.; Lambry, J.-C.; Bohn, B.; Poyart, C.; Martin, J.-L. *Nat. Struct. Biol.* **1994**, *1*, 230.

(23) Franzen, S.; Bohn, B.; Poyart, C.; DePillis, G.; Boxer, S. G.; Martin, J.-L. *J. Biol. Chem.* **1995**, *270*, 1718.

(24) Mizutani, Y.; Kitagawa, T. *J. Phys. Chem. B* **2001**, *105*, 10992.

(25) Duprat, A. F.; Traylor, T. G.; Wu, G.-Z.; Coletta, M.; Sharma, V. S.; Walda, K. N.; Magde, D. *Biochemistry* **1995**, *34*, 2634.

(26) Eliezer, D.; Chung, J.; Dyson, J.; Wright, P. E. *Biochemistry* **2000**, *39*, 2894.

(27) Piro, M. C.; Militello, V.; Leone, M.; Gryczynski, Z.; Smith, S. V.; Brinigar, W. S.; Cupane, A.; Friedman, F. K.; Fronticelli, C. *Biochemistry* **2001**, *40*, 11841.

(28) Gilmanshin, R.; Gulotta, M.; Dyer, R. B.; Callender, R. H. *Biochemistry* **2001**, *40*, 5127.

(29) English, D. S.; Das, K.; Zenner, J. M.; Zhang, W.; Kraus, G. A.; Larock, R. C.; Petrich, J. W. *J. Phys. Chem. A* **1997**, *101*, 3235.

(30) Négrerie, M.; Berka, V.; Vos, M. H.; Liebl, U.; Lambry, J.-C.; Tsai, A.-L.; Martin, J.-L. *J. Biol. Chem.* **1999**, *274*, 24694.

(31) Lambright, D. G.; Balasubramanian, S.; Decatur, S. M.; Boxer, S. G. *Biochemistry* **1994**, *33*, 5518.

(32) Skilling, J. *Maximum Entropy and Bayesian Methods*; Kluwer: Dordrecht, The Netherlands, 1988.

(33) Jaynes, E. T. In *Maximum Entropy and Bayesian Methods in Applied Statistics*; Justice, J. H., Ed.; Cambridge University Press: Cambridge, 1986.

(34) Moore, E.; Gibson, Q. *J. Biol. Chem.* **1976**, *251*, 2788.

(35) Quillin, M. L.; Li, T.; Olson, J. S.; Phillips, G. N., Jr.; Dou, Y.; Ikeda-Saito, M.; Regan, R.; Carlson, M.; Gibson, Q. H.; Li, H. *J. Mol. Biol.* **1995**, *245*, 416.

(36) Hargrove, M. *Biophys. J.* **2000**, *79*, 2733.

(37) Lim, M.; Jackson, T. A.; Anfinrud, P. A. *JBIC, J. Biol. Inorg. Chem.* **1997**, *2*, 531.

(38) Srajer, V.; Teng, T.-Y.; Ursby, T.; Pradervand, C.; Zhong, R.; Adachi, S.-I.; Schildkamp, W.; Bourgeois, D.; Wulff, M.; Moffat, K. *Science* **1996**, *274*, 1726.

(39) Shreve, A.; Franzen, S.; Simpson, M.; Dyer, R. *J. Phys. Chem. B* **1999**, *103*, 7969.

(40) Cornelius, P.; Hochstrasser, R.; Steele, A. *J. Mol. Biol.* **1983**, *163*, 119.

(41) Frauenfelder, H.; Wolynes, P. G. *Science* **1985**, *229*, 337.

(42) Lambry, J.-C. *Approches Expérimentales et Théoriques de la Dynamique Fonctionelle de la Myoglobine et de l'hémoglobine: Spectroscopie Femtoseconde et Simulation de la Dynamique Moléculaire*; Université de Paris-Sud: Orsay, France, 1997.